

A Light-weight Deep Human Activity Recognition Algorithm Using Multi-knowledge Distillation

Runze Chen, *Graduate Student Member, IEEE*, Haiyong Luo, *Member, IEEE*, Fang Zhao, *Member, IEEE*, Xuechun Meng, Zhiqing Xie, and Yida Zhu

Abstract—Inertial sensor-based human activity recognition (HAR) is the base of many human-centered mobile applications. Deep learning-based fine-grained HAR models enable accurate classification in various complex application scenarios. Nevertheless, the large storage and computational overhead of the existing fine-grained deep HAR models hinder their widespread deployment on resource-limited platforms. Inspired by the knowledge distillation’s reasonable model compression and potential performance improvement capability, we design a multi-level HAR modeling pipeline called Stage-Logits-Memory Distillation (SMLDist) based on the widely-used MobileNet. By paying more attention to the frequency-related features during the distillation process, the SMLDist improves the HAR classification robustness of the students. We also propose an auto-search mechanism in the heterogeneous classifiers to improve classification performance. Extensive simulation results demonstrate that SMLDist outperforms various state-of-the-art HAR frameworks in accuracy and F1 macro score. The practical evaluation of the Jetson Xavier AGX platform shows that the SMLDist model is both energy-efficient and computation-efficient. These experiments validate the reasonable balance between the robustness and efficiency of the proposed model. The comparative experiments of knowledge distillation on six public datasets also demonstrate that the SMLDist outperforms other advanced knowledge distillation methods of students’ performance, which verifies the good generalization of the SMLDist on other classification tasks, including but not limited to HAR.

Index Terms—human activity recognition, multi-knowledge distillation, artificial neural network, inertial sensors

I. INTRODUCTION

ACCURATELY recognizing the activities and behaviors of users with the sensors integrated into the commodity smartphones plays an essential role in ubiquitous computing. The users’ HAR contexts express plentiful semantic information about their ordinary lives, which can be used in various applications, such as smart homes [1], human-computer interaction [2], health monitoring [3], and transportation schedules [4]. For this reason, there has been a lot of research on the design of HAR algorithms. Many classical HAR algorithms focus on the extraction of manually designed statistical features [5], which requires a great deal of expert knowledge and lacks

the ability to distinguish complex movement patterns (e.g., activity switches, and periodic movements). Researchers pursue smarter, more accurate, easier-to-design HAR algorithms to overcome these issues in recent years.

Deep HAR models gradually become the focus of current researchers due to their automatic extraction with generalized features and performance benefits [6]. Many researchers design deep-learning model structures specifically for HAR. The combination of convolutional neural networks (CNN) and residual neural networks (RNN) is the most traditional way to fuse spatial and temporal features in the HAR model [4], [7]–[9]. The attention mechanism [10], [11] provides HAR methods with new ideas to enrich multi-positional sensor features’ expression [12]–[14] by introducing the relations between various sensors. These approaches introduce additional knowledge by tweaking the structure of HAR models, but it tends to introduce more computational overhead. It is more appropriate to deploy models of more general simple architecture on platforms with less computational power. The convolution-based generic structures such as MobileNet [15] have large-scale applications and general optimization for various software and hardware platforms. Improving the performance of MobileNet or other generic model structures for fine-grained HAR tasks has important research implications.

We consider improving the guidance of HAR-specific knowledge on deep HAR models while avoiding structural over-engineering. Knowledge distillation (KD) [16] inspires us to distill HAR-specific knowledge to student models. The original KD method [17] distills the teacher model’s response as the soft probabilistic target. It encourages more researchers to focus on knowledge distillation. Some knowledge distillation methods, including feature-based KD methods [18] and structure-based methods [19], try to find more forms of knowledge for guiding student models. The student structures require a lot of training to adapt distilled knowledge. Existing knowledge distillation methods explore many forms of knowledge, but we need a portfolio of HAR-specific distilling techniques.

Based on the above ideas, we propose a multi-level distillation pipeline for HAR modeling called *Stage-Memory-Logits Distillation (SMLDist)*. SMLDist provides full-level distillation to build robust deep HAR algorithms. SMLDist distills three levels of knowledge: stage, memory, and logits. Stage knowledge includes the teacher’s understanding of the tendency and periodicity of motion. Memory knowledge includes the teacher’s structural knowledge of heterogeneous classifiers with their parameters. The student reuses the heterogeneous

R. Chen, F. Zhao, X. Meng, Z. Xie and Y. Zhu are with the School of Computer Science (National Pilot Software Engineering School), Beijing University of Posts and Telecommunications, Beijing 100876, China. E-mail: {chenrz925,zfsse,mxc,xzq0112,dozenpiggy}@bupt.edu.cn

H. Luo is with the Beijing Key Laboratory of Mobile Computing and Pervasive Device, Institute of Computing Technology, Chinese Academy of Sciences, Beijing 100190, China. E-mail: yhluo@ict.ac.cn

(Corresponding author: Haiyong Luo and Fang Zhao.)

classifiers of the teacher to adapt the distilled knowledge in a few epochs. SMLDist takes into account the various forms of knowledge that play an essential role in the training process of deep HAR models and thus significantly improves the recognition accuracy of plain deep HAR models with no additional overhead. We summarize the main contributions of SMLDist as follows:

- SMLDist addresses HAR scenarios' particular tendency and periodicity characteristics by performing multi-stage distillation in the time-frequency domain. Thus, it is able to improve the quality of plain convolutional models for HAR-specific time-frequency features without introducing additional structural design.
- We train and reuse heterogeneous teacher classifiers to build more diverse memory knowledge in the training process and let the gradient choose which one to retain in the inference process. By distilling diverse structures and parameters knowledge, the teacher guides the student to avoid detours in the learning progress, which boosts the training process of the student model.
- We demonstrate that the HAR model of *SMLDist* provides excellent accuracy with ideal power consumption and responsiveness. We also demonstrate the high research value of multi-knowledge fusion distillation. Experiments demonstrate that the plain convolutional backbones without additional structural design can challenge better performance than model structures designed specifically for HAR.

The remainder of this paper is organized as follows. Section II introduces related works of human activity recognition and knowledge distillation. Section III introduces methods of SMLDist. In Section IV, we perform experiments to evaluate the availability and performance of methods in SMLDist. We make conclusions and introduce future work about this paper in Section V.

II. RELATED WORK

A. Deep Learning for HAR

Deep learning methods gain success in identifying multiple complex activities. Many researchers design new architectures of deep learning models and develop databases or toolkits to recognize human activities. DeepConvLSTM [7] provides a classical method based on CNN and LSTM (Long-Short Term Memory). HAR models use the attention mechanism [10], [11] to combine spatial features and temporal features. AttnSense [12] combines CNN modules and GRU modules with the attention mechanism. SparseSense [13] integrates a linear-based sample embedding layer and segment embedding layer to recognize human activities. IndRNN [20] is a new architecture of RNNs with independent neurons in the same layer. B. Zhao et al. [21] apply the IndRNN module to identify human activities. They use all temporal features and frequency features computed by FFT (Fast Fourier Transform) and feed them into IndRNN layers to perceive the long-term human activity pattern. J.-H. Choi et al. [22], [23] design EmbraceNet to extract correlated information between different modalities

of sensors. S. Liu et al. [14] integrate global attention mechanisms to fuse sensor features and use GRU modules to extract temporal features.

The above architectures achieve promising results on various datasets. However, the computational ability constrain the application of those elaborate models such as embedded devices or low-cost computers. At the cost of complex model structures, the generality of models is lost on top of the enhancement of special HAR tasks. How to build efficient and lightweight neural network models based on a universal neural network architecture becomes a valuable problem.

B. Knowledge Distillation

Knowledge distillation plays a vital role in upgrading lightweight models for better performance. According to the distilled forms of knowledge in the deep models [16], we can divide KD into response-based KD [17], [25], feature-based KD [26], and structure-based KD [27], [28].

The distillation of model responses leads to the concept of knowledge distillation. Hinton et al. [17] popularize the idea of knowledge distillation formally in 2015. The vanilla knowledge distillation transfers the logits in the teacher-student architecture. Z. Meng et al. [25] design a conditional loss function, which uses the hard label instead of the soft target when the teacher model predicts incorrectly. Xu et al. [26] analyze the relationship between logits distillation and label smoothing. Knowledge of neurons or features in deep models' intermediate layers is another commonly distilled form of knowledge. Romero et al. [29] use hint feature distillation to convert wide and deep models into thinner and deeper ones. Neuron selectivity transfer [30] uses MMD loss [31] to metric the distance in Gaussian space between the hint features in the teacher and student models. Similarity-preserving KD [18] distills the similarity matrix of intermediate neurons from the teacher to the student. Factor transfer [32] designs an encoder-decoder-styled module to extract the factor of the teacher model's intermediate features and uses an encoder for the student model to mimic the factor from the teacher model. Knowledge of structures and parameters arouse attention recently with a wealth of pre-trained information. T. Li et al. [27] distill the intermediate convolutional layers to the student models and use the point-wise convolution layers to establish inter-layer compatibility. C. Li [28] use KD to distill the structural knowledge to neural search space to boost the searching efficiency of neural blocks.

To the best of our knowledge, there is a lack of knowledge distillation studies specifically designed for HAR. Knowledge distillation is a general model training paradigm with high efficiency, which evolves the quality of plain model structures. Plain convolutional backbones provide a wide range of services. Many hardware and software platforms adapt and accelerate those structures. The potential of knowledge distillation provides options for building HARs based on universal lightweight model architecture. An essential problem is how to harmonize more forms of implicit HAR knowledge to guide student models.

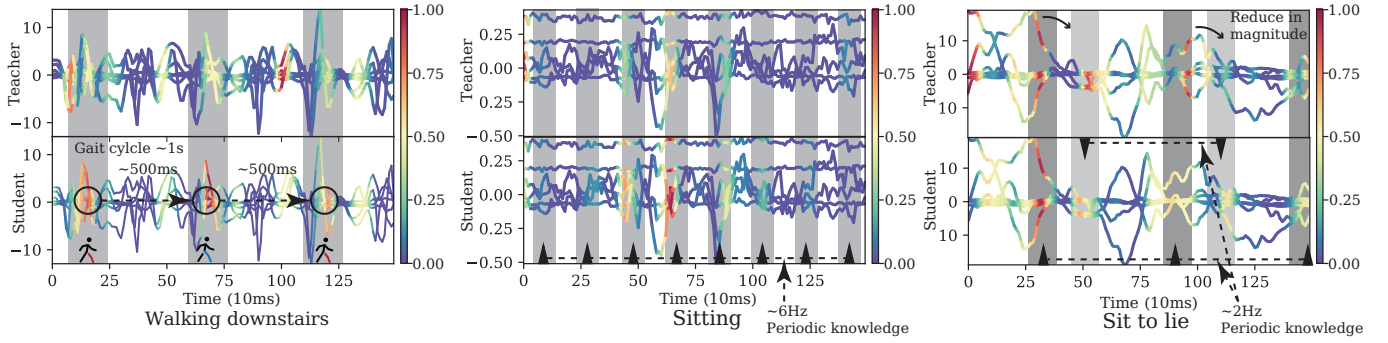


Fig. 1. Implicit frequency domain knowledge in HAR tasks. The color of raw sensor signal demonstrates the CAM [24] of SMLDist models (the model focus on signals with warmer colors and ignores signals with colder colors). Grey bar demonstrates the implicit periodical rule of human activities, e.g. walking periodicity.

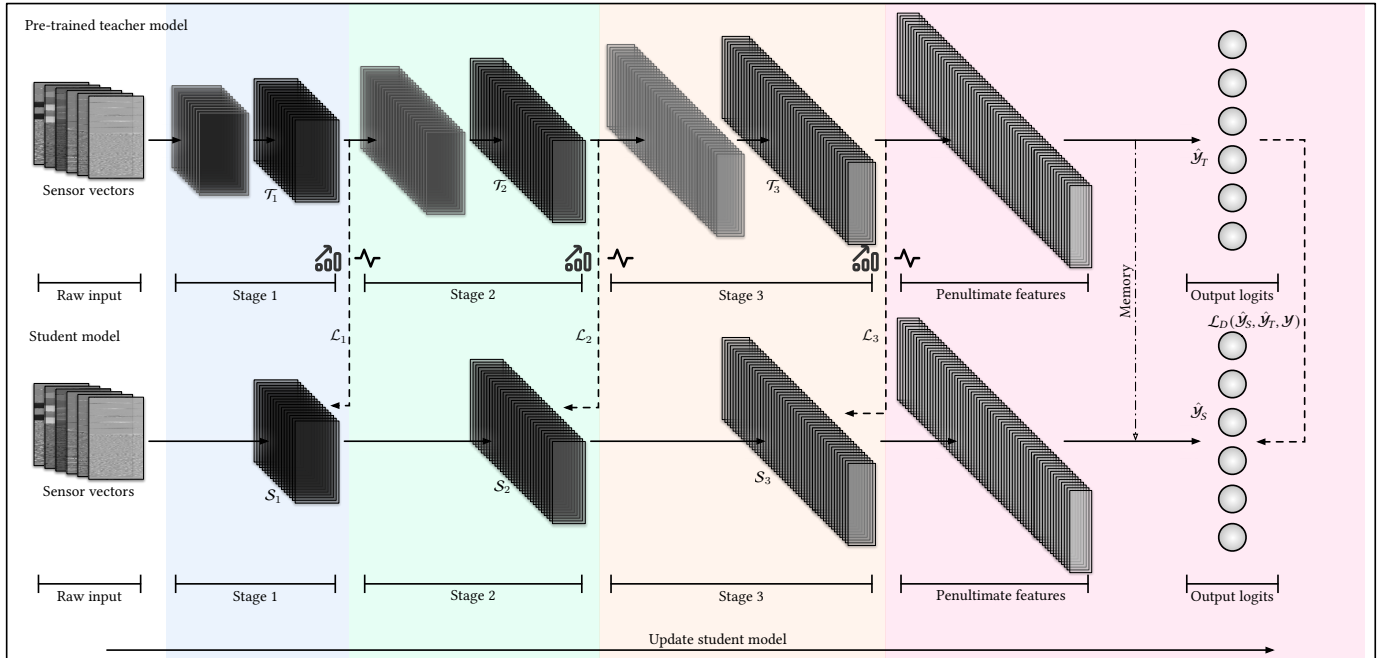


Fig. 2. The pipeline of Stage-Memory-Logits Distillation (SMLDist) for human activity recognition.

III. THE PIPELINE OF SMLDIST

In this section, we present the proposed methods of Stage-Memory-Logits Distillation (SMLDist) in detail. We first introduce the problem definitions and notations. In the order of Stage-Memory-Logits Distillation, we will introduce stage distillation, memory distillation, and logits distillation in the following sections. Figure 2 displays the pipeline of stage distillation and logits distillation to build a model with 4 stages (3 stages for representations and 1 final stage for logits).

SMLDist is a HAR modeling method based on multi-knowledge distillation. HAR model is a function $f: \mathcal{X} \rightarrow \mathcal{Y}$ mapping the raw sensor signal vectors \mathcal{X} to the final class logits \mathcal{Y} , which is the most critical part of the whole method. We predict and classify human activity through the HAR method on each temporal window on the sensor signal. For example, for the i -th window in the whole dataset, the raw signal vectors should be \mathcal{X}_i , and the class logits \mathcal{Y}_i . The collection of all participating human activity classification is

$C = \{c_i\}_{i=1}^n$. We usually use the softmax function $\sigma(\cdot)$ to map the class logits \mathcal{Y} to the class probability vector $P = (P_{c_1}, \dots, P_{c_n})$. To balance the HAR model's accuracy and efficiency, we perform stage knowledge distillation on the deep vanilla model and design the self-adaptive intuition-memory model to upgrade the model's recognition efficiency.

A. Stage Knowledge for HAR

Stage knowledge is hierarchical and highly dependent on the model architecture. Deep neural networks naturally have multiple stages internally. Student models mimic the features of the teacher models in stage order. It allows the teacher models to guide the student models' direction of optimization hierarchically, thus avoiding stuck in local optima due to limitations of training target. Introducing the implicit information acquired by the teacher model can avoid the detouring phenomenon in students' training process.

Through the lens of the teacher and student models, we are able to observe the periodicity and tendency characteristics

Algorithm 1 Stage distillation

Require: Dataset X , teacher $f_T = f_{T_1} \circ f_{T_2} \circ \dots \circ f_{T_n} \circ \mathcal{H}_T$,
 distilling optimizer O_i and loss function L_i in stage i .

Ensure: Student $f_S = f_{S_1} \circ f_{S_2} \circ \dots \circ f_{S_n} \circ \mathcal{H}_S$.

- 1: Initialize model f_S .
 - 2: **for** stage $i = 1, 2, \dots, n$ **do** ▷ Stage i .
 - 3: Let $F_T = f_{T_1} \circ \dots \circ f_{T_i}$ and $F_S = f_{S_1} \circ \dots \circ f_{S_i}$.
 - 4: **for** each epoch until F_S performs well **do**
 - 5: **for** each batch \mathcal{X} in X **do**
 - 6: $\mathcal{T}_i = F_T(\mathcal{X})$
 - 7: $\mathcal{S}_i = F_S(\mathcal{X})$
 - 8: Back-propagate with $L_i(\mathcal{S}_i, \mathcal{T}_i)$.
 - 9: Optimize F_S with $O_i(\nabla F_S)$.
 - 10: **end for**
 - 11: **end for**
 - 12: **end for**
-

implied in HAR samples. As displayed in Figure 1, the comparison of CAM (Class Activation Map) [24] highlights the interest points of the model’s stage 1 features. The 3 sensor samples include ”walking downstairs”, ”sitting” and ”sit to lie” in HAPT [33] dataset. The activity ”walking downstairs” has a typical periodic nature with a movement tendency. The teacher model focuses on localized high-frequency features. The activity ”Sitting” and activity ”Sit to lie” also have implicit frequency relations in the features. Human activity has distinct frequency characteristics. Evidently, the teacher model focus on local features with high frequency. On that basis, the student model needs to explore the periodicity of the sample further.

Assume that a model $f = f_1 \circ \dots \circ f_n \circ h$ consists of n stages, the i -th stage f_i extracts hidden features with different scales of perceptive fields, and the final layer h of the model classifies activities based on the features extracted from previous stages. When i increases, the stage f_i can perceive features on a larger temporal scale. The classifier uses the perceived features from the previous stages for the final classification. The feature $\mathcal{T}_i = (f_{T_1} \circ \dots \circ f_{T_i})(\mathcal{X})$ produced by stage i of the teacher model guides the student model how the corresponding stage extracts features $\mathcal{S}_i = (f_{S_1} \circ \dots \circ f_{S_i})(\mathcal{X})$. In stage distillation, features $\mathcal{T}_i \in \mathbb{R}^{C_i \times L_i}$ from the teacher model constrain the corresponding features $\mathcal{S}_i \in \mathbb{R}^{C_i \times L_i}$ strictly by guiding the student stages $(f_{S_1} \circ \dots \circ f_{S_i})(\cdot)$ to mimic the mapping $\mathcal{X} \rightarrow \mathcal{T}_i$ with the loss L_i ,

$$\mathcal{L}_i = \underbrace{\frac{1}{C_i \times L_i} \|\text{rfft}(\mathcal{T}_i) - \text{rfft}(\mathcal{S}_i)\|_2}_{\text{Periodic term}} + \underbrace{\frac{1}{C_i \times L_i} \|\mathcal{T}_i - \mathcal{S}_i\|_2}_{\text{Tendency term}}, \quad (1)$$

where $\text{rfft}(\cdot)$ is the one dimensional Fourier transform of real-valued input. As in Algorithm 1, the student begins the learning process for the next stage at the end of each stage.

The teacher model has pre-learned temporal characteristics of human activity. Intuitively, human activity has periodicity and tendency in the representation of sensor sequences. Convo-

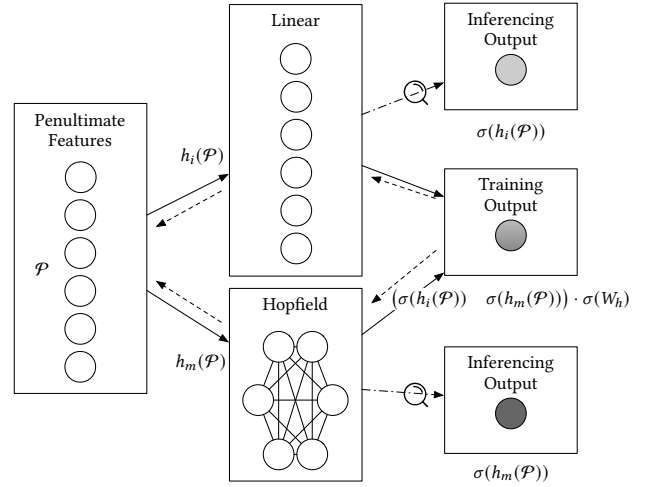


Fig. 3. Competitive training and automatic search of classifiers. In the SMLDist pipeline, the gradient tweaks the importance of each classifier, so that we select the classifier with the best importance to deploy in the final model.

lutional networks can still preserve temporal characteristics in the intermediate stages due to their structural characteristics. It means that we can deconstruct the intermediate-stage features of the convolutional network with different knowledge in the time domain and the frequency domain, respectively. Based on the distilled frequency-domain knowledge, the student model notices gait switching, an intuitive representation of walking activity. Also, the student model focuses on the low-frequency relationship apparently in the samples of activity ”Sitting” and activity ”Sit to lie” in Figure 1. The tendency term in L_i indicates the similarity of the distribution of \mathcal{T}_i and \mathcal{S}_i in the time sequence, which represent the similarity of dynamic tendency. Periodic knowledge can help students understand the tendency of data from the perspective of periods. So we introduce an additional periodic term to distill the frequency domain knowledge of the intermediate-stage features.

The training progress is progressive in SMLDist. Students have the same learning goal at each stage: to be as consistent as possible with their teacher. Staged learning objectives prevent student models from detouring for localized features. We consider classifier training as the final learning stage. The final stage determines the model’s ability to relate the high-dimensional features with class distribution, which is the key to the classification task. Therefore we combine memory distillation with logits distillation to improve the final stage of learning specifically.

B. Memory Knowledge & Auto-search of Heterogeneous Heads for Teachers and Students

The classifier of a deep neural network plays a key role in specific tasks. The overall memory of the classifier consists of the structure of the classifier as well as the parameters. For the characteristics of HAR, we explored the knowledge of structure and parameters for the classifier. The shortcoming of feature-based distillation is that students lack the ability to make decisions based on mimicking teachers’ features. To solve this problem, we introduce multiple heterogeneous

Algorithm 2 Memory & logits distillation of the final stage

Require: Dataset X with labels Y , teacher $f_T = f_{T_1} \circ f_{T_2} \circ \dots \circ f_{T_n} \circ \mathcal{H}_T$, student $f_S = f_{S_1} \circ f_{S_2} \circ \dots \circ f_{S_n} \circ \mathcal{H}_S$ pre-trained by stage distillation, distilling optimizer O_i and loss function $L = \mathcal{L}_D$.

Ensure: Student f_S .

- 1: Clone memory from \mathcal{H}_T to \mathcal{H}_S . ▷ Memory distillation
 - 2: **for** each epoch until F_S performs well **do**
 - 3: **for** each batch \mathcal{X}, \mathcal{Y} in X, Y **do**
 - 4: $\hat{\mathcal{Y}}_T = f_T(\mathcal{X})$
 - 5: $\hat{\mathcal{Y}}_S = f_S(\mathcal{X})$
 - 6: Back-propagate with $L(\hat{\mathcal{Y}}_S, \hat{\mathcal{Y}}_T, \mathcal{Y})$. ▷ Logits distillation
 - 7: Optimize F_S with $O_i(\nabla f_S)$.
 - 8: **end for**
 - 9: **end for**
 - 10: $h = \mathcal{H}_{S \arg\max(\hat{q}_{\mathcal{H}_S})}$. ▷ Auto-search.
 - 11: Replace \mathcal{H}_S with h in f_S .
-

classifiers to the model, leading them to compete in the training process. We integrate a modern Hopfield-based classifier [34] to compete with the plain linear classifier to provide heterogeneity between different classifiers as displayed in Figure 3. Theoretically, for each available classifier h in the set \mathcal{H} , the probability of them being the best choice is q_h . To solve the approximation \hat{q}_h of this probability, we set a learnable weight $\mathcal{W}_h \in \mathcal{W}$ for each h and they satisfy $\hat{q}_h = \sigma(\mathcal{W}_h | \mathcal{W})$, where σ is soft-max function. In the training process, we use the composed response $\hat{\mathcal{Y}}$ of all $h \in \mathcal{H}$ as

$$\hat{\mathcal{Y}} = \sum_{h \in \mathcal{H}} h(\mathcal{P}) \hat{q}_h, \quad (2)$$

where $\mathcal{P} = (f_1 \circ \dots \circ f_n)(\mathcal{X})$. In Figure 3, \hat{q}_h satisfies $\hat{q}_h \sigma(\mathcal{W}_h)$. The classifier with the better expressive ability for the specific HAR task gradually gains higher probability \hat{q}_h in the optimization process. We consider that the probability \hat{q}_h reflects the importance of the classifier.

In the final stage, the student no longer mimics the features extracted by the teacher but directly inherits the teacher’s memory. With inherited memory, we can fine-tune the student to adapt the classifier to the whole model, which usually requires a few epochs. After the fine-tuning process, we select the classifier with the highest estimated importance and remove other redundant classifiers. We also distill logits knowledge into the student in the fine-tuning process. The inherited memory and soft targets bridge the gap between learned representation and unexplored class distribution as displayed in Algorithm 2.

C. Logits Knowledge

Vanilla knowledge distillation [17] transfers the generalization ability from a cumbersome model to a smaller model by distilling the *logits knowledge* predicted by the teacher model to the smaller model. Teachers provide students with more

domain-specific knowledge to solve practical problems. The soft target contains more information than raw one-hot labels because of the hidden relations between classes. The classes are not independent of each other. The soft targets can explain more ignored hidden similarities between classes explained by the teacher model. In the vanilla class probability distillation, we name the output class logits as $\hat{\mathcal{Y}}_T$, and the corresponding probabilities are $P(\hat{\mathcal{Y}}_T)_c$. For a class logits $\hat{\mathcal{Y}}$, we calculate the probability $P(\hat{\mathcal{Y}})_c$ by using soft-max method σ . The vanilla class probability distillation uses both the soft target provided by the cumbersome teacher model and the manually labeled hard target. When distilling the soft target to the student model, the training loss \mathcal{L}_{KD} is combined with the cross-entropy between predicted logits $\hat{\mathcal{Y}}_S$ and soft target $\hat{\mathcal{Y}}_T$ as well as the cross-entropy between predicted logits $\hat{\mathcal{Y}}_S$ and hard ground-truth one-hot label \mathcal{Y} . The Equation 3 displays the combined loss \mathcal{L}_H of the vanilla class probability distillation:

$$\mathcal{L}_H(\hat{\mathcal{Y}}_S, \hat{\mathcal{Y}}_T, \mathcal{Y}) = \mathcal{L}_{CE}(\hat{\mathcal{Y}}_S, \mathcal{Y}_i) + \lambda \mathcal{L}_{CE}\left(\frac{\hat{\mathcal{Y}}_S}{\tau}, \frac{\hat{\mathcal{Y}}_T}{\tau}\right) \quad (3)$$

where \mathcal{L}_{CE} is the cross-entropy function, the temperature τ is the relaxation ratio, and the parameter λ is the weight between the influence of the hard label and the soft target.

Logits distillation ensures the semantic learning goals of the student model. The hard one-hot labels are not always ground truth in the real situation [26]. Manually labeled hard labels may introduce new noise for the HAR tasks. The movement features of the user can include many patterns of activity. For example, when running upstairs, the user’s activity state should be a combination of several simple activities, including jumping, running, or sometimes walking. The one-hot method to express the actual activity possibility value may ignore some fundamental activities. When the state is labeled as ”going upstairs”, other related activities such as ”walking” or ”running” should also gain certain possibilities. However, one-hot labeled logits cannot express those relatively secondary activity classes. Therefore, a harder label may be more likely to train over-fitted activity recognizing models [35].

The soft targets provided by the teacher model reveal the implicit inter-class correlations. However, the teacher model can not always provide the right prediction on the possible human activity class. So we use a conditional control technique $Q(\cdot)$ to assume that the manually labeled class can guide the student model [25], and the c -th element of controlled probability provided by the teacher model is $Q(\hat{\mathcal{Y}}_T)_c$,

$$R(\hat{\mathcal{Y}}_T)_c = \begin{cases} \gamma, & c = \arg\max \mathcal{Y} \text{ and } c \neq \arg\max \hat{\mathcal{Y}}_T \\ P(\hat{\mathcal{Y}}_T)_c, & \text{otherwise} \end{cases}, \quad (4)$$

$$Q(\hat{\mathcal{Y}}_T) = \sigma(R(\hat{\mathcal{Y}}_T)),$$

where γ is the hardness factor of $R(\cdot)$, and the controlled probability $Q(\hat{\mathcal{Y}}_T)$ corrects the effects of wrong labeled class and smooths the probability distribution of soft targets. Finally, we use $\mathcal{L}_D(\cdot)$ as the loss function to train the front-end classifier of the student model after training previous stages,

$$\begin{aligned} \mathcal{L}_D(\hat{\mathcal{Y}}_S, \hat{\mathcal{Y}}_T, \mathcal{Y}) = & - \left(\sum_{i=1}^C \mathcal{Y}_i \log(P(\hat{\mathcal{Y}}_S)_i) \right. \\ & \left. + \lambda \sum_{i=1}^C Q\left(\frac{\hat{\mathcal{Y}}_T}{\tau}\right)_i \log(P\left(\frac{\hat{\mathcal{Y}}_S}{\tau}\right)_i) \right). \end{aligned} \quad (5)$$

SMLDist, including stage distillation, memory distillation, and logits distillation, is a robust knowledge distillation pipeline to improve the HAR performance of plain convolutional deep models. The multi-knowledge distillation can significantly improve the HAR performance of lightweight models.

IV. EXPERIMENTAL EVALUATION

We evaluate and analyze SMLDist using various extensive experiments on public HAR datasets. In this section, we experimentally demonstrate that SMLDist can achieve well performance and prove the importance of multi-knowledge distillation for HAR.

A. Prerequisites

We conduct performance evaluation on six HAR datasets, including RealWorld-HAR [36], HAPT [33], HTC-TMD [37], UCI-HAR [38], DSADS [39]–[41], REALDISP [42], [43]. Those datasets are all collected through embedded devices or wearable devices on various positions of users. We will also conduct certain specific analyses on specific datasets. The overall information of those 6 datasets is in Table I.

*RealWorld-HAR dataset*¹ covers 8 sensors, including acceleration, GNSS, gyroscope, light, magnetic field, and sound level data collected on different body positions, including chest, forearm, head, shin, thigh, upper arm, and waist. However, we only select acceleration, gyroscope, and magnetic field to evaluate SMLDist. RealWorld-HAR collects 8 types of activities, including climbing stairs down and up, jumping, lying, standing, sitting, running/jogging, and walking from 15 projects (age 31.9 ± 12.4 years old, height 173.1 ± 6.9 cm, weight 74.1 ± 13.8 kg, 8 males and 7 females). In this paper, the training set consists of 13 subjects (age 39.0 ± 23.0 years old, height 173.0 ± 10.0 cm, weight 74.5 ± 20.5 kg, 7 males and 6 females), and the validation set consists of 2 projects (age 26 and 30, height 183cm and 165cm, weight 78kg and 66kg, 1 male and 1 female). The maximum sample rate of raw sensor signals is 49.95Hz, and the final sample rate of aligned sensor signals is 45Hz. We use 5 seconds as the sample window size when pre-processing the RealWorld-HAR dataset’s sensor signals. RealWorld-HAR builds a complete dataset of motion and position with abundant subjects and environments in real-world conditions.

*HAPT dataset*² consists of 3 static postures (standing, sitting, lying), 3 dynamic postures (walking, walking downstairs, and walking upstairs), and 6 postural transitions (stand-to-sit, sit-to-stand, sit-to-lie, lie-to-sit, stand-to-lie, and lie-to-stand),

a total of 12 activities. All the sensor signals (acceleration and gyroscope) are collected from 30 volunteers (age 19–48 years) wearing a smartphone (Samsung Galaxy S II) on their waist. The sample rate of raw sensor signals is 50Hz, and we randomly divide the dataset into a training set (70% of volunteers) and a validation set (other 30% of volunteers). It’s harder to classify the transition classes for HAR models than its elder version, UCI-HAR dataset.

*UCI-HAR dataset*³ only consists of 6 basic activities (standing, sitting, lying, walking, walking downstairs, and walking upstairs). Similarly, the sample rate of sensor signals is also 50Hz. Nevertheless, the window size of each sample is 2.56 seconds.

HTC-TMD dataset implements a data collection Android application for 274 participants to divide their transportation status into 10 modes with many real-time samples. The 10 modes include still (107 hours), walking (121 hours), running (61 hours), bike (78 hours), motorcycle (134 hours), car (209 hours), bus (69 hours), metro (95 hours), train (67 hours), and high-speed railway (91 hours). All the participants cover different genders (60% male and 40% female), builds, and ages (20 to 63 years old). In this paper, we selected 70% of samples randomly in the dataset as the training samples and the other 30% of samples as the validating samples.

*DSADS dataset*⁴ contains sensor signals of 19 activities performed by 8 subjects (4 female, 4 male, between the ages 20 and 30). The subjects perform the activities in their style. So there are inter-subject variations in the speeds and amplitudes of some activities between data collected from different subjects. The sample rate of sensor signals is 25Hz, and each sample is segmented into 5 seconds. In this paper, we select samples of 2 subjects randomly as validating sets.

*REALDISP dataset*⁵ collects sensor signals including acceleration, gyroscope, magnetic, and quaternion values on realistic displacements (right lower arm, right upper arm, back, left upper arm, left lower arm, right calf, right thigh, left thigh, and left calf). The dataset includes a wide range of physical activities and participants (17 subjects). The 33 dynamic activities in the dataset are more nuanced than other datasets in various positions. The dataset builds on the concepts of ideal placement, self-placement, and induced displacement. In the scenario of ideal placement, sensors are displaced strictly on ideal positions by the instructors. The training set consists of all samples of ideal displacement. Self-displacement introduces the error caused by the subjective cognition of the participants without explicit instruction. And induced-displacement introduces the error caused by instructors’ intentional mispositioning of sensors. We use samples of the other two scenarios as the evaluating set. The REALDISP dataset emphasizes robustness for HAR models due to the error of wearing position in reality.

The benchmark based on six datasets can evaluate HAR models about their universality, robustness, and compatibility.

³<https://archive.ics.uci.edu/ml/datasets/Human+Activity+Recognition+Using+Smartphones>

⁴<https://archive.ics.uci.edu/ml/datasets/Daily+and+Sports+Activities>

⁵<https://archive.ics.uci.edu/ml/datasets/REALDISP+Activity+Recognition+Dataset>

¹https://sensor.informatik.uni-mannheim.de/index.html#dataset_realworld

²<https://archive.ics.uci.edu/ml/datasets/Smartphone-Based+Recognition+of+Human+Activities+and+Postural+Transitions>

TABLE I
DESCRIPTION OF SIX PUBLIC HUMAN ACTIVITY RECOGNITION DATASETS.

Name	Subjects	Activities	Body positions	Sensors	Sample Rate	Window size
RealWorld-HAR	15	8	7	3	45Hz	5 seconds
UCI-HAR	30	6	2	2	50Hz	2.56 seconds
HTC-TMD	224	10	3	3	47Hz	5 seconds
MHEALTH	10	12	2	2	50Hz	5 seconds
HAPT	30	12	1	2	50Hz	3 seconds
DSADS	8	19	5	3	50Hz	5 seconds
REALDISP	17	33	9	3	50Hz	3 seconds

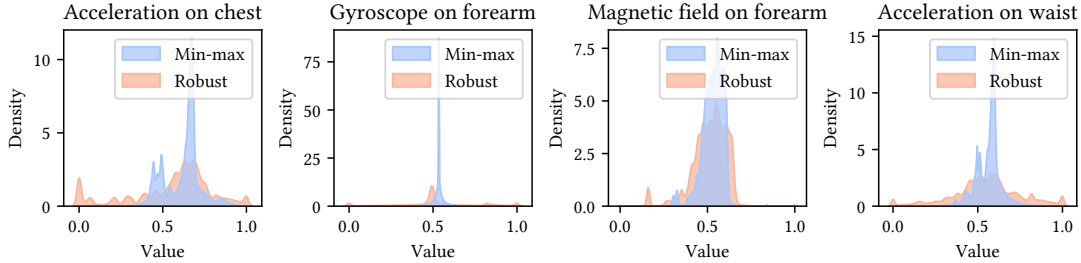


Fig. 4. Kernel distribution estimation of sensor samples in RealWorld-HAR dataset processed by minimum-maximum scaling and robust scaling.

Sensor values can fluctuate abnormally as outliers due to system errors in the MEMS sensors. These outliers can make the numerical distribution in the normal range very dense to be distinguished by the model. When normalizing the raw sensor data by the minimum-maximum scaling method displayed in Equation 6, normal values are clustered too densely in a range rather than distributed relatively evenly throughout the numerical distribution.

$$S_{minmax}(\mathcal{X}) = \frac{\text{clip}(\mathcal{X}, \min(\mathcal{X}), \max(\mathcal{X}))}{\max(\mathcal{X}) - \min(\mathcal{X})}. \quad (6)$$

We use the robust scaling method displayed in Equation 7 to avoid the significant noise introduced by the absolute boundary of raw sensor data.

$$\begin{aligned} IQR(\mathcal{X}) &= Q_3(\mathcal{X}) - Q_1(\mathcal{X}) \\ L_{lower}(\mathcal{X}) &= Q_1(\mathcal{X}) - 1.5 \cdot IQR(\mathcal{X}) \\ L_{upper}(\mathcal{X}) &= Q_3(\mathcal{X}) + 1.5 \cdot IQR(\mathcal{X}) \\ S_{robust}(\mathcal{X}) &= \frac{\text{clip}(\mathcal{X}, L_{lower}(\mathcal{X}), L_{upper}(\mathcal{X}))}{4 \cdot IQR(\mathcal{X})}, \end{aligned} \quad (7)$$

where Q_1 is the first quartile of raw sensor value \mathcal{X} , Q_3 is the third quartile of raw sensor value \mathcal{X} , and IQR is the inter-quartile range of raw sensor value \mathcal{X} . As displayed in Figure 4, we evaluate the distributions of samples normalized by the minimum-maximum scaling and the robust scaling RealWorld-HAR dataset. We use the modules of each sensor vector to display distributions. Ignoring the effects of extreme maximum-minimum scaled normalization can result in an overly dense distribution of the results. An overly dense distribution may increase the difficulty of the model sensing input feature samples. We use robust scaling to process sensor data in experiments mentioned in the following sections. We set each batch's size of training and validating samples to

TABLE II
EVALUATION ENVIRONMENTS OF SMLDIST.

Type	Information			
Server	GPU	Model	Frequency	Memory
		Intel Xeon Gold 6230	2.10GHz	187GiB
	CPU	Model	Performance	Memory
		NVIDIA Tesla V100S	130TFLOPS	32GiB
Operating system			Architecture	
CentOS Linux 7.4.1708			amd64	
Embedded device	GPU	Model	Frequency	Memory
		NVIDIA Carmel	2.30GHz	32GiB
	CPU	Model	Performance	Memory
		NVIDIA Volta	11TFLOPS	32GiB
Operating system			Architecture	
Ubuntu 18.04.5 LTS			aarch64	

256, the learning rate to 1×10^{-4} , and use the Ranger [44] algorithm to optimize the model. We use Python to build all the modeling and evaluating code and implement the models based on PyTorch [45] 1.7.1. We perform all modeling and most performance evaluation experiments in this section on a server cluster node with NVIDIA TESLA V100S GPU and Intel Xeon Gold 6230 CPU. Also, we perform experiments of embedded platforms on an NVIDIA Jetson AGX Xavier with NVIDIA Carmel ARM v8.2 64-Bit CPU and NVIDIA Volta GPU (with 512 NVIDIA CUDA cores and 64 Tensor cores). In particular, both CPU and GPU share the same memory of 32GB in NVIDIA Jetson AGX Xavier.

In the subsequent experiments, we will use accuracy and F1 macro score to indicate the performance of HAR models. The calculation of the F1 macro score is defined as

$$F1 = 2 \cdot \frac{\text{Precision} \cdot \text{Recall}}{\text{Precision} + \text{Recall}}, \quad (8)$$

where $\text{Precision} = \frac{TP}{TP+FP}$, $\text{Recall} = \frac{TP}{TP+FN}$, TP is true positives, FP is false positives, and FN is false negatives. We

also evaluate the scale of parameters and multiply accumulates (MACs), representing the model’s storage overhead and computational overhead of deep learning operations. In addition, we will use the daily average energy consumption of the model on the NVIDIA Jetson AGX Xavier platform as well as the sample energy consumption as the energy consumption metric.

B. Auto-search of Classifiers

We evaluate the estimated importance and predicted probability of the pre-trained teacher model and its student on the RealWorld dataset. Figure 5 displays these results. The validation sets used to evaluate the auto-searched head consist of continuous activities collected on 2 subjects (samples from #0 to #559 are collected on subject #14 in the RealWorld dataset. Other samples are collected on subject #15 in the RealWorld dataset). All the samples collected on the same subject are temporally continuous.

The learned \hat{q}_h of the classifier based on the Hopfield network increases while the weight of the linear classifier decreases. Figure 5a displays the Hopfield classifier’s softmax self-adaptive weights and the linear classifier when training the teacher model. The dashed vertical line annotates the epoch in which the model has the best performance. Figure 5b displays the Hopfield classifier’s softmax self-adaptive weights and the linear classifier when training the student model. The Hopfield classifier’s importance decreases continuously when training the teacher model and the student model, which means the linear classifier’s importance decreases as stored information in the Hopfield classifier increases under this condition. The student inherits the teacher’s memory as well as the teacher’s learning direction. We use only 1 epoch to fine-tune the student models in SMLDist. During the fine-tuning process, the tendency of the classifier’s importance no longer changes significantly.

The fusion of heterogeneous classifiers helps the learning of the classification task, but we can fish out the best of the best. Figure 5c displays all samples’ softmax output logits in the student model’s Hopfield classifier’s validation set. Figure 5d displays corresponding logits from the student model’s linear classifier. Comparing 5c with 5d, the Hopfield classifier can better predict a well-trained model than the linear classifier. Figure 5e displays the fused logits processed by softmax of all samples in the validation set from the Hopfield classifier and the student model’s linear classifier. Figure 5f displays the ground truth of activity in the validation set. The training process uses the fused logits as the model’s output, which is commonly affected by the linear and Hopfield classifiers. In Table III, "H" means using a Hopfield classifier independently when training and predicting, "L" means using a linear classifier independently, which is equal to the vanilla MobileNet V3 model, "A" means using the auto-selected classifier. "H+L" is the weighted fusion of the Hopfield and linear classifiers. In this scenario, the advantage of the head with higher \hat{q}_h is significant.

In conclusion, classifiers with higher estimated importance probability can provide better performance. A more complex classifier does not necessarily mean that it can provide better

TABLE III
ABLATION EVALUATION OF CLASSIFIER’S AUTO-SEARCH.

Dataset	Metric	H	L	H+L	A
RealWorld-HAR	Accuracy (%)	84.43	89.16	95.65	95.73
	F1 Macro (%)	77.37	85.14	94.73	94.84
UCI-HAR	Accuracy (%)	95.75	95.07	95.79	96.06
	F1 Macro (%)	95.69	94.94	95.68	95.94
HTC-TMD	Accuracy (%)	92.98	92.85	93.10	93.18
	F1 Macro (%)	92.71	92.56	92.76	92.87
HAPT	Accuracy (%)	88.18	90.58	90.65	93.02
	F1 Macro (%)	72.89	72.79	74.85	82.78
DSADS	Accuracy (%)	80.70	84.07	97.54	97.81
	F1 Macro (%)	77.24	81.55	97.55	97.82
REALDISP	Accuracy (%)	91.40	92.72	93.49	94.00
	F1 Macro (%)	92.11	92.17	93.19	93.79

performance. Automatic search according to the classifier’s importance is a good choice.

C. Human Activity Recognition

We conduct a series of experiments to evaluate the performance of SMLDist. The performance comparison of classification among various state-of-the-art methods and the model produced by SMLDist is displayed in Table IV. The models produced by SMLDist are based on a backbone of MobileNet V3 [15]. Both performance and efficiency are evaluation indicators of different methods. The goal of SMLDist is to find a balance between efficiency and performance. In Table IV, we perform the experiments on the six public datasets mentioned above to compare the vanilla MobileNet V3 models built by SMLDist with other well-designed architectures. As Table IV displayed, the models produced by SMLDist achieve a better performance of accuracy and F1 macro score than other baseline methods.

The SMLDist models outperform other methods with reasonable overhead. GlobalFusion has a smaller scale of parameters and MACs. However, it has a more latent capacity to improve robustness in more demanding conditions. For example, transitions between activities are hard to recognize, and the error in transitions may cause a sharp drop in the F1 macro score. As displayed in Table I, samples in RealWorld-HAR dataset have the most channels of sensors. A growing number of sensors may cause an increase in the computational and spatial overhead of the HAR model. The balance between efficiency and performance is essential to improve the robustness of the HAR model. The method based on recurrent layers, such as IndrRNN, needs more parameters and more computation resources to apply recurrent operations. In the RealWorld-HAR dataset, IndrRNN’s parameters reach 2100.6331 million, and MACs reach 2102.7232 million. Other methods combining convolutional operations and recurrent operations enable the recurrent layers to focus more on perceiving temporal patterns instead of extracting many redundant features. Those models combined with recurrent operations and convolutional operations usually design submodels for each position’s sensor in their architecture. This strategy is

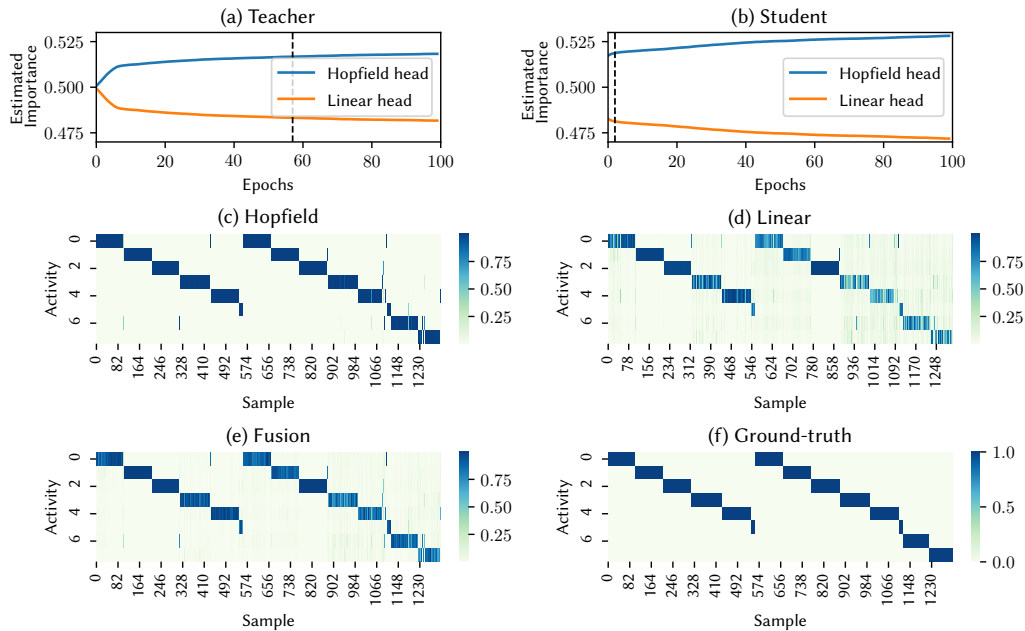


Fig. 5. Evaluation of estimated importance \hat{q}_h and predicted probability \hat{Y} of the model trained on RealWorld-HAR dataset. (a), (b) demonstrate the tendency of \hat{q}_h in SMLDist training process. (c), (d), (e), and (f) demonstrate the sample classification in time order. We can see the importance of the evaluation and selection of classifiers according to (c).

usable but improves the computational overhead dramatically. GlobalFusion has good performance and small computational overhead on most datasets. But its parameters reach 1531.4923 million and its MACs reach 1500.1324 million on the REALDISP dataset. Because of the large memory overhead of the model trained on REALDISP, the IndRNN model trained on REALDISP dataset’s performance and energy cost is not available. However, we use MobileNet V3 as the backbone structure to produce the evaluation of SMLDist, which is constructed by convolutional operations entirely. The evaluated models can get better accuracy than other models, and the increase of sensors would not cause an apparent increase in computational overheads. As a modeling pipeline based on knowledge distillation, SMLDist can also be used to build HAR models based on other backbone architectures.

To examine the energy and time overhead of the models produced by SMLDist, we deploy the models into an NVIDIA Jetson AGX Xavier and use them to predict on validating sets of all six public datasets. We measure the actual energy cost of the embedded device when the device is free. Moreover, we measure the energy cost and executing time when predicting the whole validating set of those public datasets. The difference between the predicted energy cost and the free energy cost is the real energy cost consumed by the model. As displayed in Table IV, the longest consumed time per sample when predicting with the sensor configured like the REALDISP dataset is 11.582 milliseconds. Because the REALDISP dataset captures 9 IMU sensor positions, there are more channels of sensor signals fed into the model. So the model configured on the REALDISP dataset consumes more energy than other models. Because of the limited GPU memory resource, we cannot deploy IndRNN models trained

on REALDISP dataset and RealWorld-HAR dataset on the embedded device to evaluate energy and time cost. As evaluated in the above experiments, the evaluated models produced by SMLDist can be deployed into an embedded device with reasonable energy and time cost. The evaluated models cost less than $2 W \cdot h/\text{day}$ on all evaluated datasets, which has better performance and efficiency than other models. In the large transportation mode dataset of HTC, we find ambiguity among motorcycle and bike modes. Motorcycle mode also has ambiguity with car mode. Bus mode is more challenging to recognize than other modes. In REALDISP dataset, the raw sensor values are continuous, and walking samples are far more than samples of other activities. The quantitative imbalance among different activities increases the difficulty of classification. The F1 macro score displayed in Table IV exclaims that the evaluated models provided by SMLDist have better classification robustness than other state-of-the-art models.

D. Knowledge Distillation for HAR

We evaluate the performance, including accuracy and F1 macro score of student models with different compression ratios. We use the same configurations of the teacher models to compress the student models. We use RealWorld-HAR dataset and HAPT dataset to evaluate the performance variation caused by the parameters’ compression and multiply accumulates (MACs). With the spatial and temporal overhead compression, we find that the student models’ performance decrease is small and reasonable, as shown in Figure 6. We annotate the performance of the typical teacher model as the horizontal dashed line in Figure 6. On the RealWorld-HAR dataset, the self-distilled model and models with a higher com-

TABLE IV
PREDICTING PERFORMANCE AND ENERGY & TIME COST COMPARISON OF STATE-OF-THE-ART HAR MODELS ON PUBLIC DATASETS.

Method	Dataset	Accuracy (%)	F1 Macro (%)	MACs (M)	Parameters (M)	Time cost (ms/sample)	Energy cost ($mW \cdot h/sample$)	Energy cost ($W \cdot h/day$)
DeepConv-LSTM [7]	RealWorld-HAR	76.72	66.34	14.3203	0.4144	14.479	0.0288	0.4978
	UCI-HAR	90.77	90.80	10.4268	1.9041	2.816	0.0055	0.1873
	HTC-TMD	78.54	77.95	11.4250	0.3293	4.344	0.0106	0.1839
	HAPT	84.55	70.71	7.3044	0.1955	2.861	0.0070	0.2024
	DSADS	65.83	65.89	8.0150	0.8862	3.509	0.0072	0.1248
	REALDISP	84.61	83.14	14.5689	1.5883	13.341	0.0935	2.6933
AttnSense [12]	RealWorld-HAR	90.61	89.95	189.3646	12.3379	12.525	0.0243	0.4194
	UCI-HAR	94.29	94.10	12.8616	2.5653	11.028	0.0193	0.6529
	HTC-TMD	91.45	90.98	10.5904	2.0591	23.318	0.0469	0.8102
	HAPT	87.61	74.84	12.6488	0.9057	10.455	0.0203	0.5855
	DSADS	80.61	80.62	192.6510	3.8641	85.395	0.1437	2.4838
	REALDISP	88.35	87.36	430.0884	12.3149	88.268	0.1559	4.4890
SparseSense [13]	RealWorld-HAR	90.15	83.58	75.8809	69.4538	19.870	0.0535	0.9242
	UCI-HAR	92.56	92.51	14.4920	13.3184	4.411	0.0105	0.3538
	HTC-TMD	87.09	86.52	10.9658	10.0449	4.142	0.0101	0.1742
	HAPT	86.25	77.04	7.3247	6.7329	10.455	0.0203	0.5855
	DSADS	73.73	70.61	53.9532	49.5548	13.114	0.0343	0.5932
	REALDISP	89.23	88.01	194.2680	89.1294	19.721	0.1005	2.8939
IndRNN [8]	RealWorld-HAR	83.66	53.50	2102.7232	2100.6331	-	-	-
	UCI-HAR	94.29	94.09	22.2980	22.0839	40.312	0.2892	9.7604
	HTC-TMD	90.71	90.45	46.3340	46.0250	42.563	0.2362	4.0818
	HAPT	82.46	58.81	111.1662	110.6870	62.914	0.2079	5.9886
	DSADS	74.17	73.90	888.1407	443.1107	233.728	1.8976	32.7912
	REALDISP	-	-	1501.8984	1500.1324	-	-	-
EmbraceNet [22], [23]	RealWorld-HAR	83.59	78.86	704.8512	566.6437	45.519	0.2248	3.8852
	UCI-HAR	94.53	94.52	73.3457	59.5125	6.854	0.0270	0.9115
	HTC-TMD	87.05	86.47	108.6073	87.6933	9.013	0.0393	0.6795
	HAPT	88.72	77.77	44.4001	36.1818	5.241	0.0197	0.5678
	DSADS	74.78	73.04	517.4861	208.8154	21.272	0.0883	1.5252
	REALDISP	87.71	86.40	569.8615	458.9135	38.641	0.1773	5.1073
Global-Fusion [14]	RealWorld-HAR	94.12	93.44	148.2688	1.5519	29.726	0.1454	2.5121
	UCI-HAR	95.86	95.82	158.3610	13.9316	8.449	0.0284	0.9585
	HTC-TMD	91.92	91.46	27.3844	0.6172	9.047	0.0315	0.5447
	HAPT	85.40	56.59	23.3884	0.6106	29.011	0.0720	2.0728
	DSADS	82.59	82.17	741.0103	28.7801	19.035	0.0744	1.2852
	REALDISP	91.25	89.90	1531.4923	54.6268	23.677	0.1100	3.1667
SMLDist	RealWorld-HAR	95.73	94.84	96.5486	19.1775	13.282	0.0339	0.9768
	UCI-HAR	96.06	95.94	34.0904	9.2028	8.653	0.0209	0.6013
	HTC-TMD	93.18	92.87	71.5737	3.3807	11.090	0.0240	0.4139
	HAPT	93.02	82.78	51.8479	3.7800	14.626	0.0302	0.8692
	DSADS	97.81	97.82	320.0500	18.5336	13.684	0.0385	0.6654
	REALDISP	94.00	93.79	233.2098	20.3682	11.582	0.0341	0.9827

pression ratio have better performance than the original teacher model on accuracy and F1 macro score. The F1 macro score on the HAPT dataset of the self-distilled model and models with larger compression ratios are higher than the F1 macro score of the teacher model. The smallest student model’s performance trained without SMLDist on those 2 datasets is listed as the figure’s horizontal dotted line. The student models with the highest compression ratio on 2 datasets both get apparent improvement than the model trained independently with the same configurations. Also, using SMLDist as the self-distilling technique can improve the performance of the trained model.

Different KD pipelines have different performances on HAR problems. We evaluate various knowledge-distilling pipelines with state-of-the-art in Table V. To compare the performance of different KD pipelines, we ensure all the teacher and student models in different KD pipelines have the environmental configuration (structure, compression ratio, and dataset). We

evaluate the raw mode of training the student model. In the raw mode, we train the student model independently. The student models trained by KD pipelines perform better than the raw student model under most conditions. The experiments display that SMLDist has better robustness when compressing the deep models. The performances of student models powered by SMLDist usually have less loss than models trained by other KD pipelines. Under some more demanding conditions, Models compressed by other KD pipelines dramatically influence the F1 macro score of the predictions. As the most classical baseline of KD methods, vanilla KD improves the performance of the lightweight student model better than the independently trained model with equal computational overheads on most of the datasets. However, the effects of vanilla KD have a significant loss on HTC-TMD, DSADS, and REALDISP. Part of mispredicted soft targets may mislead the student model and have adverse effects. CKD enhances

TABLE V
 PREDICTING PERFORMANCE COMPARISON OF VARIOUS KD METHODS AND ABLATION EVALUATION OF SMLDIST WITH EQUAL COMPRESSION RATIO ON PUBLIC DATASETS.

Method	Accuracy (%)						F1 Macro (%)					
	<i>RealWorld-HAR</i>	<i>UCL-HAR</i>	<i>HTC-TMD</i>	<i>HAPT</i>	<i>DSADS</i>	<i>REALDISP</i>	<i>RealWorld-HAR</i>	<i>UCL-HAR</i>	<i>HTC-TMD</i>	<i>HAPT</i>	<i>DSADS</i>	<i>REALDISP</i>
Raw Student	82.52	94.64	92.73	84.15	95.53	93.00	82.27	94.58	92.36	42.13	95.51	92.86
Vanilla KD [17]	90.31	94.70	92.95	85.15	93.86	91.69	86.09	94.67	92.70	43.92	93.27	93.12
CKD [25]	93.21	95.08	92.41	91.12	96.05	93.48	89.29	95.03	92.08	71.49	95.84	93.22
FitNets [29]	90.08	95.52	88.53	86.98	95.26	91.85	84.14	95.46	81.50	43.75	95.17	91.37
NST [30]	92.37	94.94	86.13	84.38	95.88	92.83	89.10	94.89	79.37	44.32	95.76	91.95
FNKD [26]	86.56	94.94	92.11	87.90	96.93	92.84	80.86	94.83	91.72	56.27	96.86	92.56
SPKD [18]	86.18	95.15	92.40	86.14	94.65	93.20	69.78	95.11	92.02	45.05	94.63	92.67
FT [32]	84.27	95.76	92.15	86.75	95.00	92.46	68.87	95.70	91.79	44.92	94.91	91.86
SMLDist w/o S	90.31	94.33	87.86	89.96	89.08	92.37	83.88	94.24	77.17	77.53	88.66	91.29
SMLDist w/o M	94.20	95.86	91.92	91.79	96.75	93.94	93.50	95.77	80.15	80.31	96.67	93.54
SMLDist w/o L	94.96	95.72	92.92	91.85	96.93	93.61	94.37	95.58	93.53	80.41	96.92	93.32
SMLDist w/o S, M	87.02	94.71	91.39	89.50	88.60	93.67	74.06	94.65	90.87	74.93	87.95	93.51
SMLDist w/o S, L	91.83	94.84	92.62	86.96	88.42	92.73	87.57	94.72	91.34	73.67	87.23	92.26
SMLDist w/o M, L	95.50	95.92	90.26	91.98	97.25	93.64	94.81	95.81	81.04	79.87	97.38	93.43
SMLDist	95.73	96.06	93.18	93.02	97.81	94.00	94.84	95.94	92.87	82.78	97.82	93.79

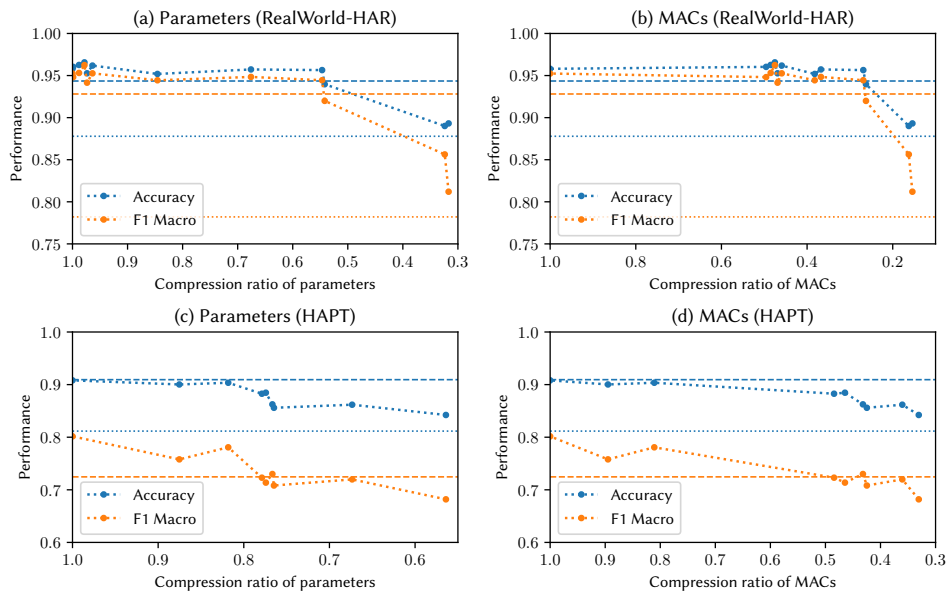


Fig. 6. Performance curve of student models with decreasing compression ratio.

the quality of distilled soft targets by mapping the wrong soft targets to the hard labels. So the CKD has a considerable improvement on most of the datasets. Feature normalization of KD (FNKD) may not always have a positive effect. On a larger-scaled dataset, such as RealWorld-HAR and HTC-TMD, the student models trained by FNKD have a slight decrease in performance compared with the models trained by vanilla KD. As displayed in Table V, SMLDist is more robust in the HAR tasks under more conditions. We use 100 epochs to train the above baseline KD pipelines, but for SMLDist, we only use 5 epochs to achieve the performance in Table V. Both the representation of the model and the efficiency of distillation

have reasonable improvements.

All parts of SMLDist are critical. We conduct ablation evaluations on SMLDist with the same configuration of the student models and the teacher models. As displayed in Table V, we perform experiments on different combinations of stage distillation, memory distillation, and logits distillation, respectively. Removing stage distillation causes the most significant performance loss to the whole SMLDist technique. Stage distillation enables the most significant enhancement of all the raw students, which proves the stability of stage distillation. But the independent stage distillation performs worse than the raw student model and SMLDist. The introduction of memory

distillation and logits distillation enhances the stability of independent stage distillation. The experiment also proves that directly transferring parameters from teacher to student, such as memory distillation, is not desirable. Memory distillation is usually available as a complement to stage distillation. We perform all SMLDist’s ablation evaluations with fine-tuning of 5 epochs. Reusing the classifiers boosts the fine-tuning speed of the student models, which avoids the detour in the student’s learning process. Conversely, we also find that too much fine-tuning degrade the model’s performance after reusing teachers’ classifiers. Logits distillation brings a small performance improvement over stage-memory distillation, which introduce more implicit information than the hard labels. Ablation evaluations demonstrate that the cooperation of stage distillation, memory distillation, and logits distillation can lead to better generality and accuracy of the lightweight model.

V. CONCLUSION AND FUTURE WORK

This paper describes the framework of SMLDist, a structural distilling pipeline designed for HAR. SMLDist builds a multi-level pipeline of knowledge distillation with the cooperation of stage distillation, memory distillation, and logits distillation. We demonstrate that cooperation of multiple HAR-specific knowledge can provide better HAR performance than single form of knowledge distillation.

Stage distillation is feature-level knowledge distillation between models based on the balance of periodic knowledge and movement tendency knowledge. It introduces the frequency-domain relationship as periodic knowledge. Thus the student model strengthens the perception of the periodic characteristics of HAR samples. We also design an automatic search mechanism for the optimal classifier by learnable importance for HAR models. The auto-search mechanism improves the accuracy of the lightweight HAR model significantly. A combination of the semantic knowledge from logits distillation and the auto-searched memory knowledge makes up for the lack of the stage distillation process to achieve better robustness of the deep HAR model. SMLDist is an effective method to build HAR models based on universally deployed structures such as MobileNet. Models optimized by SMLDist can work with reasonable energy costs on embedded devices.

There are also lots of challenges for human-centered perception. Various deep-learning applications for on-the-go deployments still present large application challenges. There are still many scenario limitations for inertia-based fine-grained activity recognition. Both the behavioral differences among users and the huge cost of acquiring tagged data also hinder the implementation of inertial-based activity recognition. Vision-based intelligent perception still suffers from high model computation and storage overhead. Designing new lightweight models and proposing more efficient model compression methods are fascinating research directions.

ACKNOWLEDGMENT

This work was supported in part by the National Key Research and Development Program under Grant

2018YFB0505200, the National Natural Science Foundation of China under Grant 61872046 and 62261042, the Key Research Projects of the Joint Research Fund for Beijing Natural Science Foundation and the Fengtai Rail Transit Frontier Research Joint Fund under Grant L221003, Beijing Natural Science Foundation under Grant 4212024 and 4222034, the Strategic Priority Research Program of Chinese Academy of Sciences under Grant XDA28040000, the Key Research and Development Project from Hebei Province under Grant 21310102D, the Fundamental Research Funds for the Central Universities under Grant 2022RC13 and the Open Project of the Beijing Key Laboratory of Mobile Computing and Pervasive Device, Institute of Computing Technology, Chinese Academy of Sciences.

REFERENCES

- [1] T. van Kasteren, G. Englebienne, and B. J. A. Kröse, “An activity monitoring system for elderly care using generative and discriminative models,” *Pers. Ubiquitous Comput.*, vol. 14, no. 6, pp. 489–498, 2010. [Online]. Available: <https://doi.org/10.1007/s00779-009-0277-9>
- [2] A. Almeida and A. Alves, *Activity Recognition for Movement-Based Interaction in Mobile Games*. New York, NY, USA: Association for Computing Machinery, 2017. [Online]. Available: <https://doi.org/10.1145/3098279.3125443>
- [3] L. T. Nguyen, M. Zeng, P. Tague, and J. Zhang, “Recognizing new activities with limited training data,” in *Proceedings of the 2015 ACM International Symposium on Wearable Computers, ISWC 2015, Osaka, Japan, September 7-11, 2015*, K. Mase, M. Langheinrich, D. Gatica-Perez, K. V. Laerhoven, and T. Terada, Eds. ACM, 2015, pp. 67–74. [Online]. Available: <https://doi.org/10.1145/2802083.2808388>
- [4] Y. Zhu, H. Luo, R. Chen, F. Zhao, and L. Su, “Densenetx and gru for the sussex-huawei locomotion-transportation recognition challenge,” in *Adjunct Proceedings of the 2020 ACM International Joint Conference on Pervasive and Ubiquitous Computing and Proceedings of the 2020 ACM International Symposium on Wearable Computers*, ser. UbiComp-ISWC ’20. New York, NY, USA: Association for Computing Machinery, 2020, p. 373–377. [Online]. Available: <https://doi.org/10.1145/3410530.3414349>
- [5] A. Bulling, U. Blanke, and B. Schiele, “A tutorial on human activity recognition using body-worn inertial sensors,” *ACM Comput. Surv.*, vol. 46, no. 3, jan 2014. [Online]. Available: <https://doi.org/10.1145/2499621>
- [6] L. Wang, H. Gjoreski, M. Ciliberto, S. Mekki, S. Valentin, and D. Roggen, “Enabling reproducible research in sensor-based transportation mode recognition with the sussex-huawei dataset,” *IEEE Access*, vol. 7, pp. 10870–10891, 2019. [Online]. Available: <https://doi.org/10.1109/ACCESS.2019.2890793>
- [7] F. J. Ordóñez and D. Roggen, “Deep convolutional and lstm recurrent neural networks for multimodal wearable activity recognition,” *Sensors*, vol. 16, no. 1, 2016. [Online]. Available: <https://www.mdpi.com/1424-8220/16/1/115>
- [8] B. Zhao, S. Li, and Y. Gao, “Intrnn based long-term temporal recognition in the spatial and frequency domain,” in *Adjunct Proceedings of the 2020 ACM International Joint Conference on Pervasive and Ubiquitous Computing and Proceedings of the 2020 ACM International Symposium on Wearable Computers*, ser. UbiComp-ISWC ’20. New York, NY, USA: Association for Computing Machinery, 2020, p. 368–372. [Online]. Available: <https://doi.org/10.1145/3410530.3414355>
- [9] Y. Zhu, F. Zhao, and R. Chen, “Applying 1d sensor densenet to sussex-huawei locomotion-transportation recognition challenge,” in *Adjunct Proceedings of the 2019 ACM International Joint Conference on Pervasive and Ubiquitous Computing and Proceedings of the 2019 ACM International Symposium on Wearable Computers*, ser. UbiComp/ISWC ’19 Adjunct. New York, NY, USA: Association for Computing Machinery, 2019, p. 873–877. [Online]. Available: <https://doi.org/10.1145/3341162.3345571>
- [10] V. Mnih, N. Heess, A. Graves, and K. Kavukcuoglu, “Recurrent models of visual attention,” in *Advances in Neural Information Processing Systems 27: Annual Conference on Neural Information Processing Systems 2014, December 8-13 2014, Montreal, Quebec, Canada*, Z. Ghahramani, M. Welling, C. Cortes, N. D.

- Lawrence, and K. Q. Weinberger, Eds., 2014, pp. 2204–2212. [Online]. Available: <https://proceedings.neurips.cc/paper/2014/hash/09c6c3783b4a70054da74f2538ed47c6-Abstract.html>
- [11] A. Vaswani, N. Shazeer, N. Parmar, J. Uszkoreit, L. Jones, A. N. Gomez, L. Kaiser, and I. Polosukhin, “Attention is all you need,” in *Advances in Neural Information Processing Systems 30: Annual Conference on Neural Information Processing Systems 2017, December 4-9, 2017, Long Beach, CA, USA*, I. Guyon, U. von Luxburg, S. Bengio, H. M. Wallach, R. Fergus, S. V. N. Vishwanathan, and R. Garnett, Eds., 2017, pp. 5998–6008. [Online]. Available: <https://proceedings.neurips.cc/paper/2017/hash/3f5ee243547dee91fbd053c1c4a845aa-Abstract.html>
- [12] H. Ma, W. Li, X. Zhang, S. Gao, and S. Lu, “Attnsense: Multi-level attention mechanism for multimodal human activity recognition,” in *Proceedings of the Twenty-Eighth International Joint Conference on Artificial Intelligence, IJCAI 2019, Macao, China, August 10-16, 2019*, S. Kraus, Ed. ijcai.org, 2019, pp. 3109–3115. [Online]. Available: <https://doi.org/10.24963/ijcai.2019/431>
- [13] A. Abedin, S. H. Rezaatfighi, Q. Shi, and D. C. Ranasinghe, “Sparsense: Human activity recognition from highly sparse sensor data-streams using set-based neural networks,” in *Proceedings of the Twenty-Eighth International Joint Conference on Artificial Intelligence, IJCAI-19*. International Joint Conferences on Artificial Intelligence Organization, 7 2019, pp. 5780–5786. [Online]. Available: <https://doi.org/10.24963/ijcai.2019/801>
- [14] S. Liu, S. Yao, J. Li, D. Liu, T. Wang, H. Shao, and T. Abdelzaher, “Globalfusion: A global attentional deep learning framework for multisensor information fusion,” *Proc. ACM Interact. Mob. Wearable Ubiquitous Technol.*, vol. 4, no. 1, Mar. 2020. [Online]. Available: <https://doi.org/10.1145/3380999>
- [15] A. Howard, M. Sandler, B. Chen, W. Wang, L. Chen, M. Tan, G. Chu, V. Vasudevan, Y. Zhu, R. Pang, H. Adam, and Q. Le, “Searching for mobilenetv3,” in *2019 IEEE/CVF International Conference on Computer Vision (ICCV)*, 2019, pp. 1314–1324.
- [16] J. Gou, B. Yu, S. J. Maybank, and D. Tao, “Knowledge distillation: A survey,” *Int. J. Comput. Vis.*, vol. 129, no. 6, pp. 1789–1819, 2021. [Online]. Available: <https://doi.org/10.1007/s11263-021-01453-z>
- [17] G. Hinton, O. Vinyals, and J. Dean, “Distilling the knowledge in a neural network,” 2015.
- [18] F. Tung and G. Mori, “Similarity-preserving knowledge distillation,” in *2019 IEEE/CVF International Conference on Computer Vision, ICCV 2019, Seoul, Korea (South), October 27 - November 2, 2019*. IEEE, 2019, pp. 1365–1374. [Online]. Available: <https://doi.org/10.1109/ICCV.2019.00145>
- [19] H. Chen, Y. Wang, C. Xu, C. Xu, and D. Tao, “Learning student networks via feature embedding,” *IEEE Transactions on Neural Networks and Learning Systems*, vol. 32, no. 1, pp. 25–35, 2021.
- [20] S. Li, W. Li, C. Cook, C. Zhu, and Y. Gao, “Independently recurrent neural network (indrn): Building a longer and deeper RNN,” in *2018 IEEE Conference on Computer Vision and Pattern Recognition, CVPR 2018, Salt Lake City, UT, USA, June 18-22, 2018*. IEEE Computer Society, 2018, pp. 5457–5466. [Online]. Available: http://openaccess.thecvf.com/content/_cvpr/_2018/html/Li_Independently_Recurrent_Neural_CVPR_2018_paper.html
- [21] B. Zhao, S. Li, Y. Gao, C. Li, and W. Li, “A framework of combining short-term spatial/frequency feature extraction and long-term indrn for activity recognition,” *Sensors*, vol. 20, no. 23, p. 6984, 2020. [Online]. Available: <https://doi.org/10.3390/s20236984>
- [22] J.-H. Choi and J.-S. Lee, “Embracenet for activity: A deep multimodal fusion architecture for activity recognition,” in *Adjunct Proceedings of the 2019 ACM International Joint Conference on Pervasive and Ubiquitous Computing and Proceedings of the 2019 ACM International Symposium on Wearable Computers*, ser. UbiComp/ISWC ’19 Adjunct. New York, NY, USA: Association for Computing Machinery, 2019, p. 693–698. [Online]. Available: <https://doi.org/10.1145/3341162.3344871>
- [23] J. Choi and J. Lee, “Embracenet: A robust deep learning architecture for multimodal classification,” *Inf. Fusion*, vol. 51, pp. 259–270, 2019. [Online]. Available: <https://doi.org/10.1016/j.inffus.2019.02.010>
- [24] B. Zhou, A. Khosla, A. Lapedriza, A. Oliva, and A. Torralba, “Learning deep features for discriminative localization,” in *2016 IEEE Conference on Computer Vision and Pattern Recognition, CVPR 2016, Las Vegas, NV, USA, June 27-30, 2016*. IEEE Computer Society, 2016, pp. 2921–2929. [Online]. Available: <https://doi.org/10.1109/CVPR.2016.319>
- [25] Z. Meng, J. Li, Y. Zhao, and Y. Gong, “Conditional teacher-student learning,” in *IEEE International Conference on Acoustics, Speech and Signal Processing, ICASSP 2019, Brighton, United Kingdom, May 12-17, 2019*. IEEE, 2019, pp. 6445–6449. [Online]. Available: <https://doi.org/10.1109/ICASSP.2019.8683438>
- [26] K. Xu, L. Rui, Y. Li, and L. Gu, “Feature normalized knowledge distillation for image classification,” in *Computer Vision - ECCV 2020 - 16th European Conference, Glasgow, UK, August 23-28, 2020, Proceedings, Part XXV*, ser. Lecture Notes in Computer Science, A. Vedaldi, H. Bischof, T. Brox, and J. Frahm, Eds., vol. 12370. Springer, 2020, pp. 664–680. [Online]. Available: https://doi.org/10.1007/978-3-030-58595-2_40
- [27] T. Li, J. Li, Z. Liu, and C. Zhang, “Few sample knowledge distillation for efficient network compression,” in *2020 IEEE/CVF Conference on Computer Vision and Pattern Recognition, CVPR 2020, Seattle, WA, USA, June 13-19, 2020*. Computer Vision Foundation / IEEE, 2020, pp. 14627–14635. [Online]. Available: https://openaccess.thecvf.com/content/_CVPR/_2020/html/Li_Few_Sample_Knowledge_Distillation_for_Efficient_Network_Compression_CVPR_2020_paper.html
- [28] C. Li, J. Peng, L. Yuan, G. Wang, X. Liang, L. Lin, and X. Chang, “Block-wisely supervised neural architecture search with knowledge distillation,” in *2020 IEEE/CVF Conference on Computer Vision and Pattern Recognition, CVPR 2020, Seattle, WA, USA, June 13-19, 2020*. Computer Vision Foundation / IEEE, 2020, pp. 1986–1995. [Online]. Available: https://openaccess.thecvf.com/content/_CVPR/_2020/html/Li_Block-Wisely_Supervised_Neural_Architecture_Search_With_Knowledge_Distillation_CVPR_2020_paper.html
- [29] A. Romero, N. Ballas, S. E. Kahou, A. Chassang, C. Gatta, and Y. Bengio, “Fitnets: Hints for thin deep nets,” in *3rd International Conference on Learning Representations, ICLR 2015, San Diego, CA, USA, May 7-9, 2015, Conference Track Proceedings*, Y. Bengio and Y. LeCun, Eds., 2015. [Online]. Available: <http://arxiv.org/abs/1412.6550>
- [30] Z. Huang and N. Wang, “Like what you like: Knowledge distill via neuron selectivity transfer,” *CoRR*, vol. abs/1707.01219, 2017. [Online]. Available: <http://arxiv.org/abs/1707.01219>
- [31] A. Gretton, K. M. Borgwardt, M. J. Rasch, B. Schölkopf, and A. Smola, “A kernel two-sample test,” *J. Mach. Learn. Res.*, vol. 13, no. 1, p. 723?773, Mar. 2012.
- [32] J. Kim, S. Park, and N. Kwak, “Paraphrasing complex network: Network compression via factor transfer,” in *Advances in Neural Information Processing Systems 31: Annual Conference on Neural Information Processing Systems 2018, NeurIPS 2018, December 3-8, 2018, Montréal, Canada*, S. Bengio, H. M. Wallach, H. Larochelle, K. Grauman, N. Cesa-Bianchi, and R. Garnett, Eds., 2018, pp. 2765–2774. [Online]. Available: <https://proceedings.neurips.cc/paper/2018/hash/6d9cb7de5e8ac30bd5e8734bc96a35c1-Abstract.html>
- [33] J. L. Reyes-Ortiz, L. Oneto, A. Samà, X. Parra, and D. Anguita, “Transition-aware human activity recognition using smartphones,” *Neurocomputing*, vol. 171, pp. 754–767, 2016. [Online]. Available: <https://doi.org/10.1016/j.neucom.2015.07.085>
- [34] H. Ramsauer, B. Schäfl, J. Lehner, P. Seidl, M. Widrich, L. Gruber, M. Holzleitner, M. Pavlović, G. K. Sandve, V. Greiff, D. Kreil, M. Kopp, G. Klambauer, J. Brandstetter, and S. Hochreiter, “Hopfield networks is all you need,” in *Submitted to International Conference on Learning Representations*, 2021, under review. [Online]. Available: <https://openreview.net/forum?id=TL89RnZiCd>
- [35] R. Müller, S. Kornblith, and G. E. Hinton, “When does label smoothing help?” in *Advances in Neural Information Processing Systems 32: Annual Conference on Neural Information Processing Systems 2019, NeurIPS 2019, December 8-14, 2019, Vancouver, BC, Canada*, H. M. Wallach, H. Larochelle, A. Beygelzimer, F. d’Alché-Buc, E. B. Fox, and R. Garnett, Eds., 2019, pp. 4696–4705. [Online]. Available: <http://papers.nips.cc/paper/8717-when-does-label-smoothing-help>
- [36] T. Szttyler and H. Stuckenschmidt, “On-body localization of wearable devices: An investigation of position-aware activity recognition,” in *2016 IEEE International Conference on Pervasive Computing and Communications, PerCom 2016, Sydney, Australia, March 14-19, 2016*. IEEE Computer Society, 2016, pp. 1–9. [Online]. Available: <https://doi.org/10.1109/PERCOM.2016.7456521>
- [37] M. Yu, T. Yu, S. Wang, C. Lin, and E. Y. Chang, “Big data small footprint: The design of A low-power classifier for detecting transportation modes,” *Proc. VLDB Endow.*, vol. 7, no. 13, pp. 1429–1440, 2014. [Online]. Available: <http://www.vldb.org/pvldb/vol7/p1429-yu.pdf>
- [38] D. Anguita, A. Ghio, L. Oneto, X. Parra, and J. L. Reyes-Ortiz, “A public domain dataset for human activity recognition using smartphones,” in *21st European Symposium on Artificial Neural Networks, ESANN 2013, Bruges, Belgium, April 24-26, 2013*, 2013. [Online]. Available: <http://www.elen.ucl.ac.be/Proceedings/esann/esannpdf/es2013-84.pdf>
- [39] K. Altun, B. Barshan, and O. Tunçel, “Comparative study on classifying human activities with miniature inertial and magnetic sensors,” *Pattern*

Recognit., vol. 43, no. 10, pp. 3605–3620, 2010. [Online]. Available: <https://doi.org/10.1016/j.patcog.2010.04.019>

[40] B. Barshan and M. C. Yükses, “Recognizing daily and sports activities in two open source machine learning environments using body-worn sensor units,” *Comput. J.*, vol. 57, no. 11, pp. 1649–1667, 2014. [Online]. Available: <https://doi.org/10.1093/comjnl/bxt075>

[41] K. Altun and B. Barshan, “Human activity recognition using inertial/magnetic sensor units,” in *Human Behavior Understanding, First International Workshop, HBU 2010, Istanbul, Turkey, August 22, 2010. Proceedings*, ser. Lecture Notes in Computer Science, A. A. Salah, T. Gevers, N. Sebe, and A. Vinciarelli, Eds., vol. 6219. Springer, 2010, pp. 38–51. [Online]. Available: https://doi.org/10.1007/978-3-642-14715-9_5

[42] O. Baños, M. Damas, H. Pomares, I. Rojas, M. A. Tóth, and O. Amft, “A benchmark dataset to evaluate sensor displacement in activity recognition,” in *The 2012 ACM Conference on Ubiquitous Computing, Ubicomp ’12, Pittsburgh, PA, USA, September 5-8, 2012*, A. K. Dey, H. Chu, and G. R. Hayes, Eds. ACM, 2012, pp. 1026–1035. [Online]. Available: <https://doi.org/10.1145/2370216.2370437>

[43] O. Baños, M. A. Tóth, M. Damas, H. Pomares, and I. Rojas, “Dealing with the effects of sensor displacement in wearable activity recognition,” *Sensors*, vol. 14, no. 6, pp. 9995–10023, 2014. [Online]. Available: <https://doi.org/10.3390/s140609995>

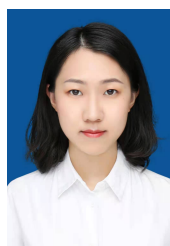
[44] H. Yong, J. Huang, X. Hua, and L. Zhang, “Gradient centralization: A new optimization technique for deep neural networks,” in *Computer Vision - ECCV 2020 - 16th European Conference, Glasgow, UK, August 23-28, 2020, Proceedings, Part I*, ser. Lecture Notes in Computer Science, A. Vedaldi, H. Bischof, T. Brox, and J. Frahm, Eds., vol. 12346. Springer, 2020, pp. 635–652. [Online]. Available: https://doi.org/10.1007/978-3-030-58452-8_37

[45] A. Paszke, S. Gross, F. Massa, A. Lerer, J. Bradbury, G. Chanan, T. Killeen, Z. Lin, N. Gimelshein, L. Antiga, A. Desmaison, A. Köpf, E. Yang, Z. DeVito, M. Raison, A. Tejani, S. Chilamkurthy, B. Steiner, L. Fang, J. Bai, and S. Chintala, “Pytorch: An imperative style, high-performance deep learning library,” in *Advances in Neural Information Processing Systems 32: Annual Conference on Neural Information Processing Systems 2019, NeurIPS 2019, December 8-14, 2019, Vancouver, BC, Canada*, H. M. Wallach, H. Larochelle, A. Beygelzimer, F. d’Alché-Buc, E. B. Fox, and R. Garnett, Eds., 2019, pp. 8024–8035. [Online]. Available: <https://proceedings.neurips.cc/paper/2019/hash/bdbca288fee7f92f2bfa9f7012727740-Abstract.html>



Fang Zhao received the B.S. degree from the School of Computer Science and Technology, Huazhong University of Science and Technology, Wuhan, China, in 1990, the M.S. and Ph.D. degrees in computer science and technology from the Beijing University of Posts and Telecommunications, Beijing, China, in 2004 and 2009, respectively. She is currently a Professor with the School of Software Engineering, Beijing University of Posts and Telecommunication. Her research interests include mobile computing, location-based services,

and computer networks.



Xuechun Meng received the B.S. degree from the School of Computer science and Technology, China University of Mining and Technology, Jiangsu, China, in 2020. She is currently studying in Beijing University of Posts and Telecommunications and is a visiting student in the Institute of Computer Technology, Chinese Academy. Her interests include: simultaneous localization and mapping, semantic segmentation.



Zhiqing Xie received the B.S. degree from the School of Computer Science and Technology, China University of Mining and Technology, Jiangsu, China, in 2020. He is working toward the M.S. degree in Beijing University of Posts and Telecommunications and is a visiting student in the Institute of Computer Technology, Chinese Academy. His research interests include: mobile computing and mobile intelligence.



Runze Chen received the B.S. degree from the School of Software Engineering, Beijing University of Posts and Telecommunications, Beijing, China, in 2019. He is working toward the Ph.D. degree in Beijing University of Posts and Telecommunications and is a visiting student in the Institute of Computer Technology, Chinese Academy. His research interests include: mobile computing, autonomous vehicles and mobile intelligence.



Haiyong Luo received the B.S. degree from the Department of Electronics and Information Engineering, Huazhong University of Science and Technology, Wuhan, China, in 1989, the M.S. degree from the School of Information and Communication Engineering, Beijing University of Posts and Telecommunication, China, in 2002, and the Ph.D. degree in computer science from the University of Chinese Academy of Sciences, Beijing, China, in 2008. He is currently an Associate Professor with the Institute of Computer Technology, Chinese

Academy of Science, China. His main research interests are location-based services, pervasive computing, mobile computing, and Internet of Things. He is a member of the IEEE.



Yida Zhu received the B.S. degree in soft engineering from the School of Software Engineering, Beijing University of Posts and Telecommunications, Beijing, China, in 2017. He is currently pursuing the Ph.D. degree with the School of Software Engineering, Beijing University of Posts and Telecommunications, and is a visiting student in the Institute of Computer Technology, Chinese Academy. His current main interests include location-based services, pervasive computing, deep learning, transfer learning, and machine learning.